J Supercond Nov Magn (2009) 22: 37–40
DOI 10.1007/s10948-008-0372-6

ORIGINAL PAPER

Electron–Phonon Interaction and Phonon Renormalization in the Lamellar Cobaltate Na_xCoO_2

A. Donkov · I. Eremin · J. Knolle · M.M. Korshunov

Received: 10 October 2008 / Accepted: 13 October 2008 / Published online: 25 October 2008

Abstract We study theoretically the electron–phonon interaction in Na_xCoO_2. For the A_{1g} and E_{1g} phonon modes found in Raman experiments, we calculate the matrix elements of the electron–phonon interaction. Analyzing the feedback effect of the conduction electrons on the phonon frequency ω, we investigate the doping dependence of these two phonon modes. Due to the momentum dependence of the electron–phonon interaction, we find the strongest renormalization of the E_{1g} mode around the Brillouin zone boundary which should be observed in the neutron scattering. At the same time, the A_{1g} mode shows the strongest coupling to the conducting electrons around the Γ point and reveals its doping dependence in the Raman experiments. Our results shed light on the possible importance of the electron–phonon interaction in the lamellar sodium cobaltates.

Keywords Electron–phonon interaction · Superconductivity · Sodium cobaltate

A. Donkov · I. Eremin (✉) · J. Knolle · M.M. Korshunov
Max-Planck-Institut für Physik komplexer Systeme,
01187 Dresden, Germany
e-mail: ieremin@mpipks-dresden.mpg.de

I. Eremin
Institute für Mathematische und Theoretische Physik,
TU Braunschweig, 38106 Braunschweig, Germany

M.M. Korshunov
Siberian Branch of Russian Academy of Sciences, L.V. Kirensky
Institute of Physics, 660036 Krasnoyarsk, Russia

1 Introduction

The discovery of superconductivity with $T_c = 4.6$ K in water intercalated sodium cobaltate, $Na_xCoO_2 \cdot yH_2O$ [1], is of great interest on its own and also because of similarities with layered cuprates. The sodium cobaltate has a quasi-two-dimensional layered structure with CoO_2 layers and rich phase diagram as a function of the Na concentration, which includes superconductivity at $x \approx 0.3$, an insulating phase at $x \sim 0.5$, and unusual magnetism for $x \geq 0.6$ [2]. In Na_xCoO_2, the Na ions reside between the CoO_2 layers, with Co ions forming a triangular lattice, and donate x electrons to the partially filled Co-$d(t_{2g})$ orbitals. Due to the presence of a trigonal crystalline electric field, the t_{2g} levels split into the higher lying a_{1g} singlet and the two lower lying e'_g states [3]. Angle-Resolved Photo-Emission Spectroscopy (ARPES) [4, 5] reveals a doping dependent evolution of the Fermi surface, which shows no sign of the e'_g hole pockets for $0.3 \leq x \leq 0.8$. The observed Fermi surface is centered around the Γ point and has mostly a_{1g} character. It has been argued that such an effect may arise due to strong electronic correlations [6, 7, 9] or Na induced disorder [8]; however, no consensus in the literature has been reached yet [10].

Despite of intensive studies of the electronic and magnetic properties little is known about the phonon excitations and their doping evolution in Na_xCoO_2. Due to the relatively low superconducting transition temperature, the possible relevance of phonons for superconductivity cannot be neglected. For example, the relevance of the electron–phonon coupling in Na_xCoO_2 to superconductivity and charge ordering has been discussed in the context of a $t-V$ model [11, 12]. In addition, due to some similarity to high-T_c cuprates the understanding of the phonon renormalization in the sodium cobaltates is of great importance.

Here, we investigate the electron–phonon interaction in the Na_xCoO_2 as a function of doping concentration for various momenta. This work compliments our previous study [13]. In particular, we concentrate on the two oxygen phonon modes with A_{1g} and E_{1g} symmetries, which were found in Raman experiments. Following the derivation of the diagonal electron–phonon matrix elements for these modes, we calculate the renormalization of the phonon frequencies by conduction electrons. Due to the structure of the electron–phonon matrix elements we obtain the strongest renormalization of the in-plane E_{1g} oxygen mode around that Brillouin zone (BZ) boundary and no renormalization at $\mathbf{q}=0$, which agrees with Raman experiments. At the same time, such a renormalization should be visible in neutron scattering and we propose to test it experimentally. Our results shed light on the possible role of the electron–phonon interaction in this compound.

2 Tight-Binding Model

To describe the electronic subsystem we use a tight-binding t_{2g}-band model with parameters (in-plane hoppings and the single-electron energies) derived previously from the *ab-initio* LDA (Local Density Approximation) calculations using projection procedure for $x=0.33$ [6].

The free-electron Hamiltonian of the t_{2g}-band model in a hole representation is given by

$$H_0=-\sum_{\mathbf{k},\alpha,\sigma}\left(\epsilon^{\alpha}-\mu\right)n_{\mathbf{k}\alpha\sigma}-\sum_{\mathbf{k},\sigma}\sum_{\alpha,\beta}t_{\mathbf{k}}^{\alpha\beta}d_{\mathbf{k}\alpha\sigma}^{\dagger}d_{\mathbf{k}\beta\sigma}, \qquad (1)$$

where $n_{\mathbf{k}\alpha\sigma}=d_{\mathbf{k}\alpha\sigma}^{\dagger}d_{\mathbf{k}\alpha\sigma}$, $d_{\mathbf{k}\alpha\sigma}$ ($d_{\mathbf{k}\alpha\sigma}^{\dagger}$) is the annihilation (creation) operator for the t_{2g}-hole with spin σ, orbital index α, and momentum $\mathbf{k}$, $t_{\mathbf{k}}^{\alpha\beta}$ is the hopping matrix element, and ϵ^{α} is the single-electron energy. To obtain the dispersion, we diagonalize the Hamiltonian (1) calculating the chemical potential μ self-consistently. Due to the nonzero interorbital hopping matrix elements, a_{1g} and e_g' bands are hybridized. However, only one of the *hybridized* bands crosses the Fermi level. We refer to the diagonalized bands as $\varepsilon_{\mathbf{k}}^{\alpha'}$ with the new orbital index α'.

3 Electron–Phonon Interaction

In analogy to previous considerations for cuprates [14, 15], we derive the electron–phonon matrix elements, $g_{\mathbf{kq}}$, for the A_{1g} and E_{1g} phonon modes depicted in Figs. 1(a) and (b). Namely, to obtain the main contribution to the diagonal (intraband) part of the electron–phonon interaction, we expand the Coulomb energy between Co and oxygen, $H_C=\frac{ee^*}{\epsilon}\sum_{i,\alpha',\sigma,\gamma}c_{i\alpha'\sigma}^{\dagger}c_{i\alpha'\sigma}(\frac{1}{|\mathbf{R}_i-\mathbf{r}_{i,\gamma}|}+\frac{1}{|\mathbf{R}_i-\mathbf{r}_{i,-\gamma}|})$, in the

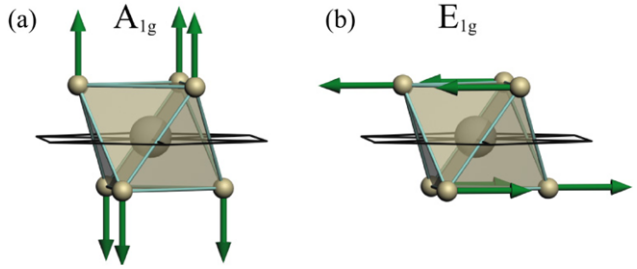

Fig. 1 (Color online) Schematic illustration of the A_{1g} (**a**) and E_{1g} (**b**) phonon modes. The *arrows* indicate the oxygen displacement in the CoO_6 octahedra

small displacements of the oxygen ions. Here, e is the electron charge, $e^*=-2e$ is the oxygen ion charge, ϵ is the dielectric constant, $\mathbf{R}_i$ are the Co ion positions, $\mathbf{r}_{i,\gamma}$ are the vector positions of the vibrating oxygens, and index γ ($-\gamma$) labels the three oxygen positions within CoO_6 unit cell above (below) the Co layer. Here, $c_{i\alpha'\sigma}^{\dagger}$ refers to the diagonal form of the Hamiltonian (1).

After introducing the creation (annihilation) operator $b_{-\mathbf{q}}^{\dagger}$ ($b_{\mathbf{q}}$) for the phonon with momentum $\mathbf{q}$, we arrive to the following form of the electron–phonon interaction

$$H_{\mathrm{el-ph}}^{\mathrm{diag}}=\sum_{\mathbf{k},\mathbf{q},\alpha',\sigma}g_{\mathbf{q}}^{\alpha'\alpha'}c_{\mathbf{k}\alpha'\sigma}^{\dagger}c_{\mathbf{k}-\mathbf{q}\alpha'\sigma}\left(b_{\mathbf{q}}+b_{-\mathbf{q}}^{\dagger}\right). \qquad (2)$$

For the sake of simplicity, we assume the diagonal electron–phonon interaction is independent on the orbital index α'. Thus, for the A_{1g} and E_{1g} optical Raman-active phonon oxygen modes, one finds $g_{\mathbf{q}}^{A_{1g}}=g_{\mathrm{diag}}^{A_{1g}}F_{\mathbf{q}}^{A_{1g}}$, $g_{\mathbf{q}}^{E_{1g}}=g_{\mathrm{diag}}^{E_{1g}}F_{\mathbf{q}}^{E_{1g}}$, where the structure factors of the electron–phonon interaction are

$$F_{\mathbf{q}}^{A_{1g}}=\cos\frac{q_1-q_2}{3}+\cos\frac{q_1+q_3}{3}+\cos\frac{q_2+q_3}{3}, \qquad (3)$$

$$F_{\mathbf{q}}^{E_{1g}}=\cos\frac{q_1-q_2}{3}-\frac{1}{2}\left[\cos\frac{q_1+q_3}{3}+\cos\frac{q_2+q_3}{3}\right]. \qquad (4)$$

Here, $q_1=(\sqrt{3}/2)q_x-\frac{1}{2}q_y$, $q_2=q_y$, $q_3=(\sqrt{3}/2)q_x+\frac{1}{2}q_y$, in units of $2\pi/a$ with a being the in-plane lattice constant, $g_{\mathrm{diag}}^{\Gamma}=-\frac{ee^*}{\epsilon}\frac{2L_{\Gamma}}{\sqrt{d^2+l^2}^3}\sqrt{\frac{\hbar}{2M\omega_{\Gamma}}}$, where ω_{Γ} is the corresponding bare phonon frequency ($\Gamma=A_{1g},E_{1g}$), $L_{A_{1g}}=d=a/\sqrt{6}$ is the distance between the Co and the oxygen plane, $L_{E_{1g}}=l=a/\sqrt{3}$ is the planar distance between Co and oxygen, and M is the oxygen mass. Assuming that in the band insulator, $Na_{x=1}CoO_2$, the renormalization of the phonons by the conduction electrons is absent, we use $\omega_{A_{1g}}=588\ \mathrm{cm}^{-1}$ and $\omega_{E_{1g}}=470\ \mathrm{cm}^{-1}$. These values are close to those obtained by the first principles calculations [16]. The resulting momentum dependence of the structure factors for the both modes is shown in Figs. 2(a) and 3(a) along the main symmetry directions on the first BZ.

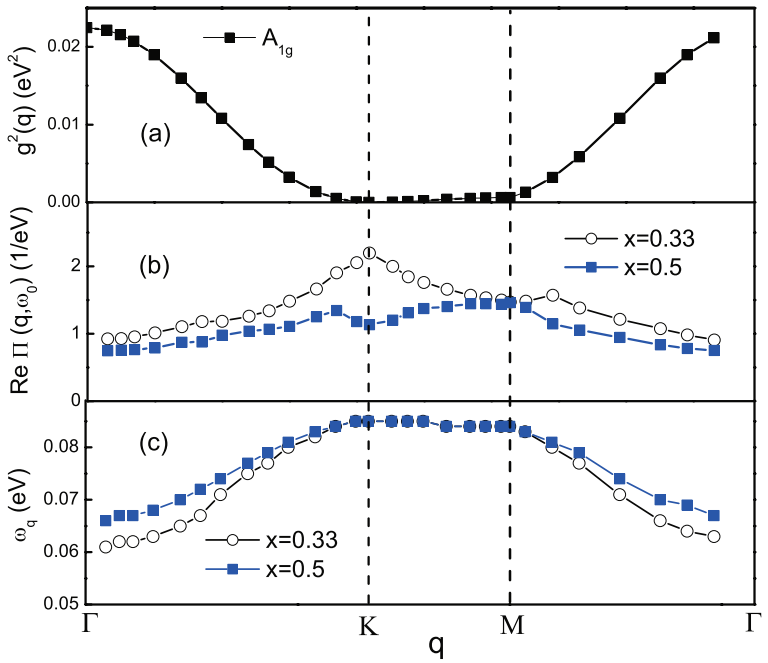

Fig. 2 (Color online) Results for the A_{1g}-phonon mode: (**a**) the calculated momentum dependence of the electron–phonon coupling, (**b**) the polarization operator at ω_0, and (**c**) the resulting phonon frequency as obtained by numerical solution of (5) with constant bare phonon frequency ω_0. We present results for two doping concentrations, $x = 0.33$ and $x = 0.5$

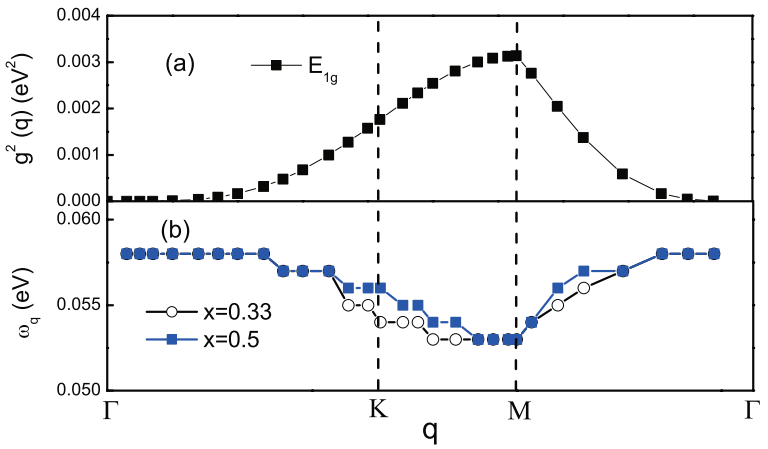

Fig. 3 (Color online) Results for the E_{1g}-phonon mode: calculated momentum dependence of (**a**) the electron–phonon coupling constant $g_{\mathbf{q}}^2$ and (**b**) the renormalized phonon frequency $\omega_{\mathbf{q}}$ for two doping concentrations, $x = 0.33$ and $x = 0.5$

Interestingly, one sees that while the $g_{\mathbf{q}}$ for the A_{1g} mode shows a maximum at the BZ center, the $g_{\mathbf{q}}$ for the E_{1g} mode vanishes there. Therefore, for $\mathbf{q} = 0$, the electron–phonon coupling for the E_{1g} channel is zero but should be the largest one around the **K** and **M** points. The situation is opposite for the A_{1g} phonon mode: the largest coupling to the conduction electrons occur in this case around the Γ point of he first BZ. This explains the doping dependence of the A_{1g} phonon mode (and the doping independence of the E_{1g} mode) observed in Raman experiments where $\mathbf{q} = 0$ point is probed [13].

In the following, we consider the renormalization of the A_{1g} and E_{1g} phonons. The corresponding Dyson equation reads:

$$D^{-1}(\mathbf{q}, \omega) = D_0^{-1}(\omega) - \left(g_{\mathbf{q}}^{\alpha'}\right)^2 \Pi(\mathbf{q}, \omega), \tag{5}$$

where $D_0(\omega) = \frac{2\omega_\Gamma}{\omega^2 - \omega_\Gamma^2 + i\delta}$ is the momentum-independent bare phonon propagator. The polarization operator is given by:

$$\Pi(\mathbf{q}, \omega) = -2 \sum_{\mathbf{k}} \frac{f(\varepsilon_{\mathbf{k}+\mathbf{q}}^{\alpha'}) - f(\varepsilon_{\mathbf{k}}^{\alpha'})}{\omega - \varepsilon_{\mathbf{k}+\mathbf{q}}^{\alpha'} + \varepsilon_{\mathbf{k}}^{\alpha'} + i\delta}, \tag{6}$$

where $f(\epsilon)$ is the Fermi function. Note that due to independence of the $g_{\mathbf{q}}$ on the internal $\mathbf{k}$ momenta we have defined the polarization operator without the g^2 multiplication. Previously, to find the renormalization of the bare phonon frequency and to compare the results to the Raman experiments we set $\mathbf{q} \to 0$ limit and solved (5) numerically as a function of the doping concentration [13]. The main contribution to the renormalization of the optical phonon modes in Raman experiments comes from the *interband* transi-

tions, i.e., terms with $g_{\mathbf{kq}}^{\alpha'\neq\beta'}$ while intraband transitions have been neglected. Here, we concentrate on the estimates of the *intraband* contribution. Thus, for the sake of simplicity, we consider only the a_{1g}-conduction band with the nearest neighbor hopping $t = 0.2$ eV. The results of our numerical calculations are shown in Figs. 2 and 3. We find that the $\mathrm{Re}\,\Pi(\mathbf{q}, \omega_0)$ is momentum dependent and at $x = 0.33$ the maximum occurs around the antiferromagnetic wave vector, $\mathbf{Q}_{\mathrm{AFM}} = \mathbf{K}$ (see Fig. 2(b)). With increasing doping toward $x = 0.5$, the nesting condition shifts away from the K point of the BZ and the overall $\mathrm{Re}\,\Pi$ decreases. This is obvious since with increasing number of carriers the system approaches the band insulator where the polarization operator is zero.

In Figs. 2(c) and 3(b), we show the resulting momentum dependence of the phonon frequencies for the A_{1g} and E_{1g} phonon modes along the main symmetry points of the first BZ. The largest softening of the A_{1g} phonon mode arises around the Γ point as we have already previously noticed [13]. At the same time, we find that the largest renormalization of the E_{1g} mode is around the M point of the BZ. Moreover, the large sensitivity of the renormalization with respect to the variation of the electron–phonon coupling constant is observed. In particular, we expect that the observed in $Na_{0.5}CoO_2$ CDW/SDW transitions should be visible in the experiments probing the phonon dispersions. This would be interesting to check experimentally.

4 Conclusion

Summarizing, we have analyzed the doping dependence of the electron–phonon interaction in Na_xCoO_2. For the two phonon modes with A_{1g} and E_{1g} symmetries we calculate the matrix elements of the electron–phonon interaction. Analyzing the feedback effect of the conduction electrons on the phonon frequency, we investigate the doping dependence of the A_{1g} and E_{1g} phonon modes. Due to the momentum dependence of the electron–phonon interaction, we find the strongest renormalization of the E_{1g} mode around the Brillouin zone boundary, which should be observed in the neutron scattering. At the same time, the A_{1g} mode shows the strongest coupling to the conducting electrons around the Γ point, and thus reveals its doping dependence in the Raman experiments.

References

1. Takada, K., Sakurai, H., Takayama-Muromachi, E., Izumi, F., Dilanian, R.A., Sasaki, T.: Nature **422**, 53 (2003)
2. Foo, M.L., Wang, Y., Watauchi, S., Zandbergen, H.W., He, T., Cava, R.J., Ong, N.P.: Phys. Rev. Lett. **92**, 247001 (2004)
3. Singh, D.J.: Phys. Rev. B **61**, 13397 (2000)
4. Hasan, M.Z., Chuang, Y.-D., Qian, D., Li, Y.W., Kong, Y., Kuprin, A., Fedorov, A.V., Kimmerling, R., Rotenberg, E., Rossnagel, K., Hussain, Z., Koh, H., Rogado, N.S., Foo, M.L., Cava, R.J.: Phys. Rev. Lett. **92**, 246402 (2004)
5. Yang, H.-B., Wang, S.-C., Sekharan, A.K.P., Matsui, H., Souma, S., Sato, T., Takahashi, T., Takeuchi, T., Campuzano, J.C., Jin, R., Sales, B.C., Mandrus, D., Wang, Z., Ding, H.: Phys. Rev. Lett. **92**, 246403 (2004)
6. Korshunov, M.M., Eremin, I., Shorikov, A., Anisimov, V.I., Renner, M., Brenig, W.: Phys. Rev. B **75**, 094511 (2007)
7. Zhou, S., Gao, M., Ding, H., Lee, P.A., Wang, Z.: Phys. Rev. Lett. **94**, 206401 (2005)
8. Singh, D.J., Kasinathan, D.: Phys. Rev. Lett. **97**, 016404 (2006)
9. Marianetti, C.A., Haule, K., Parcollet, O.: Phys. Rev. Lett. **99**, 246404 (2007)
10. Pillay, D., Johannes, M.D., Mazin, I.I., Andersen, O.K.: arXiv: 0804.3768 (unpublished)
11. Foussats, A., Greco, A., Bejas, M., Muramatsu, A.: Phys. Rev. B **72**, 020504(R) (2005)
12. Bejas, M., Greco, A., Foussats, A.: Phys. Rev. B **75**, 033101 (2007)
13. Donkov, A.A., Korshunov, M., Eremin, I., Lemmens, P., Gnezdilov, V., Chou, F.C., Lin, C.T.: Phys. Rev. B **77**, 100504(R) (2008)
14. Nazarenko, A., Dagotto, E.: Phys. Rev. B **53**, 2987(R) (1996)
15. Ovchinnikov, S.G., Schneider, E.I.: Z. Eksp. Teor. Fiz. **128**, 974 (2005) (JETP **101**, 844 (2005))
16. Li, Z., Yang, J., Hou, J.G., Zhu, Q.: Phys. Rev. B **70**, 144518 (2004)